A NOVEL APPROACH TO SOLVING THE ERW WELD ZONE

Daniele D. G. Calista
PhD Candidate CCWJ
University of Alberta

Dr. Greg R. Lehnhoff
Manager, Welding and Testing R&D
EVRAZ – North America

Prof. Umberto Prisco
Associate Professor
University of Napoli Federico II

Prof. Patricio F. Mendez
Director CCWJ
University of Alberta

CANWELD 2024
June 12, 2024

Setting context…

The General Problem

- Industry seeks the ***enabling*** of ERW products for ***harsh service*** environments
  - Hydrogen service
  - Sour gas service
  - Carbon dioxide sequestration projects

Limiting Factor

ERW products can exhibit comparatively low *toughness*.

Key Toughness Challenges

- Microstructure
- Weld seam defects
  - stringers
  - cold weld
  - **penetrators**

Can only be prevented before or during welding!

Primary Process Stages

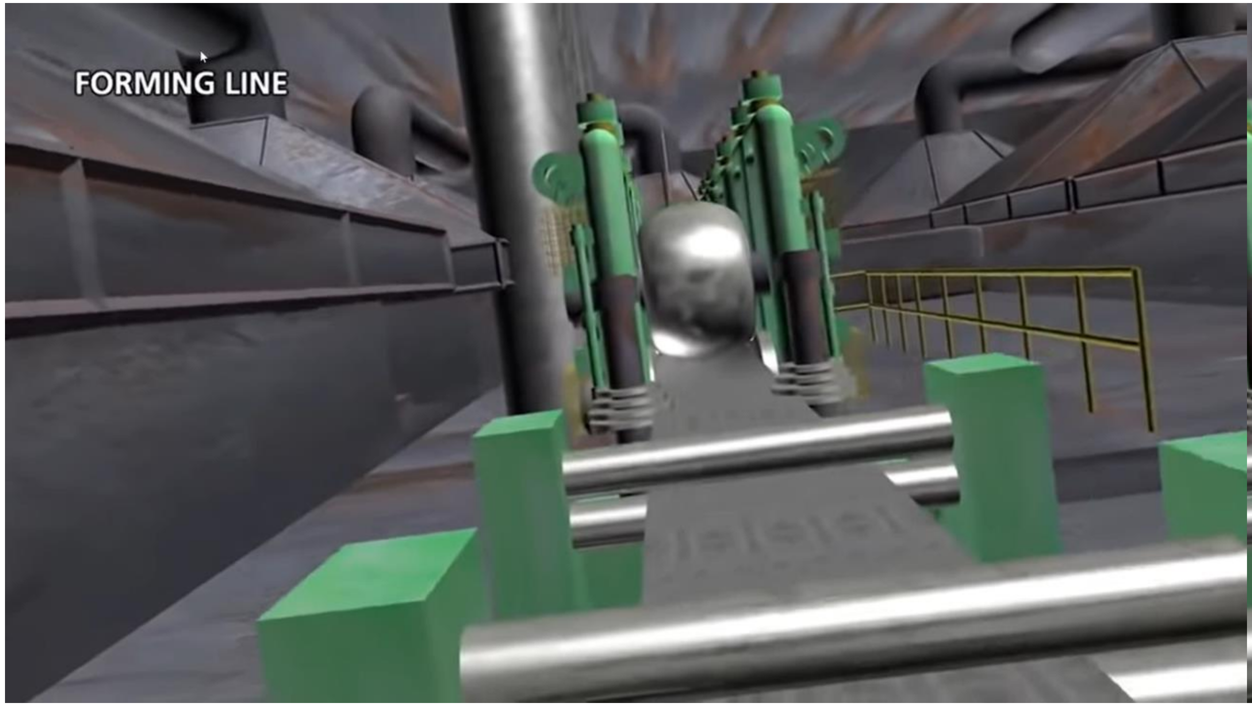

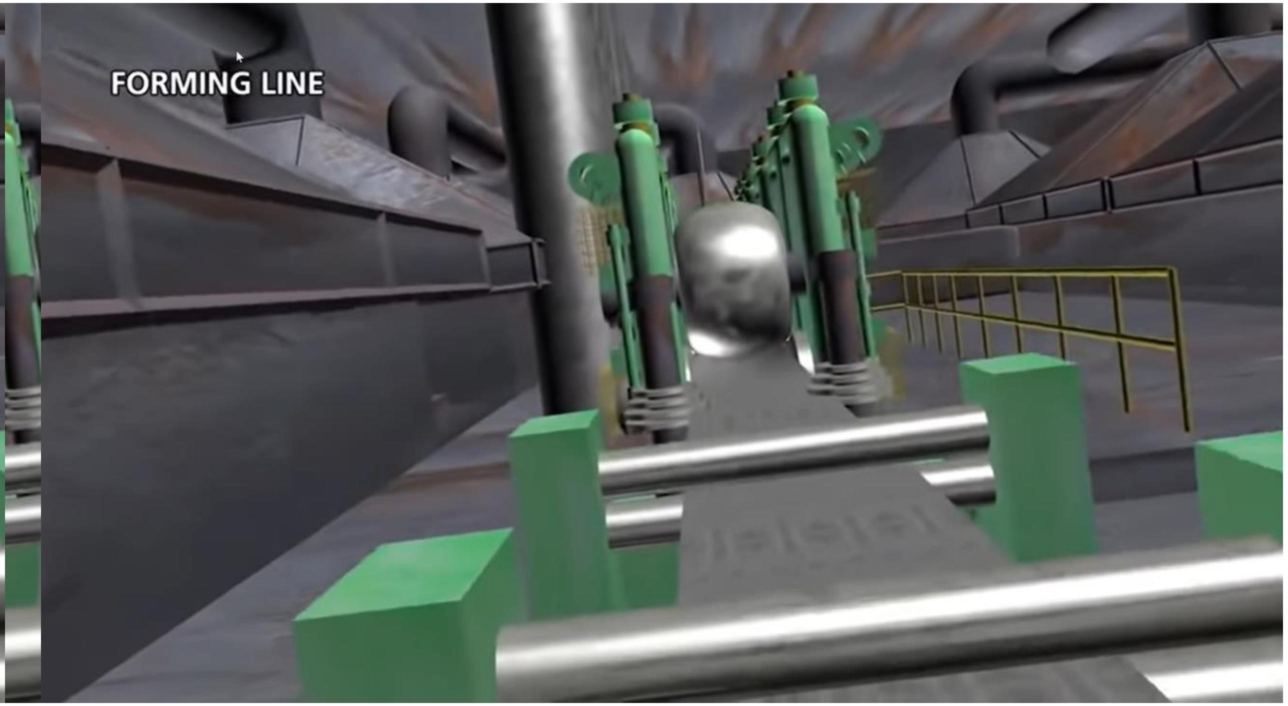

Sliding contact ERW

Skelp forming

High frequency induction welding

Videos taken from Tenaris: https://www.youtube.com/watch?v=0x1uRR9Jb34

The Scientific Problem: Penetrators

- Pervasive and distributed nature along a weld's bond line
- Penetrators are susceptible to the same microstructural effects as inclusions
- Orientation in tubular goods facilitates through-thickness propagation

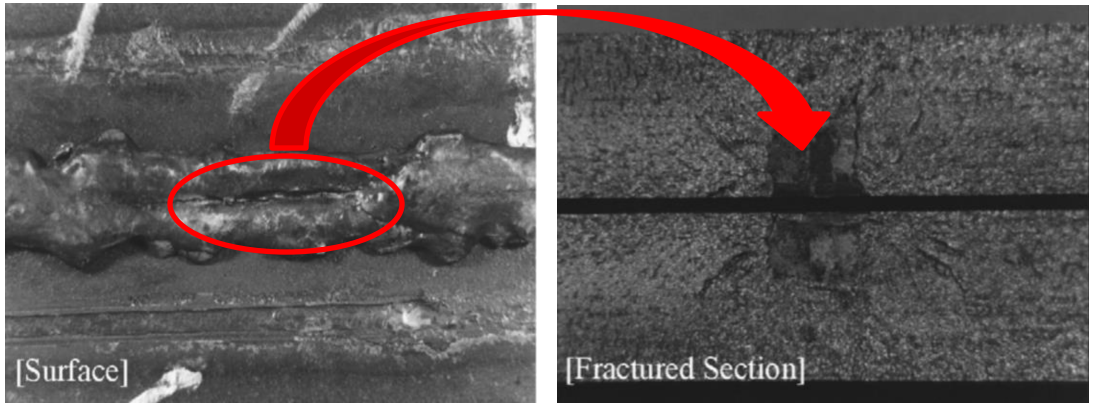

Top-down view of an ERW weld seam (left) and the corresponding bond surface after fracture containing a penetrator.
(C. M. Kim and J. K. Kim, Jan. 2009)

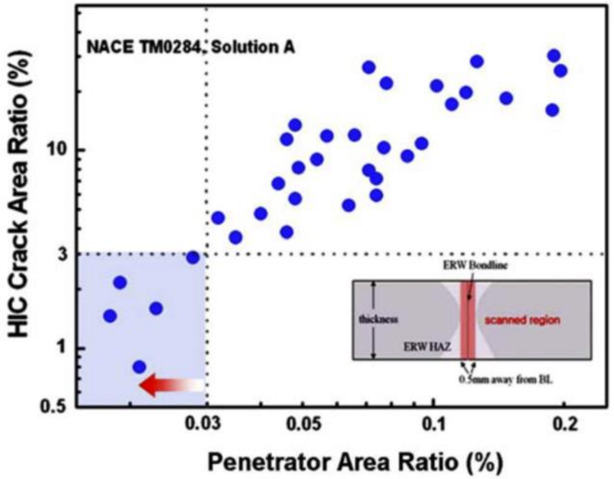

Observed hydrogen-induced-crack evolution linked to amount of penetrators.
(H. U. Hong, J. B. Lee, and H. J. Choi, 2009)

What has industry done to address penetrators?

- Full seam inspection via in-situ phased array ultr
- Closed-loop control via coupled optical & l zone

Industry lacks a physical understanding of ***why*** penetrators occur at certain welding conditions.

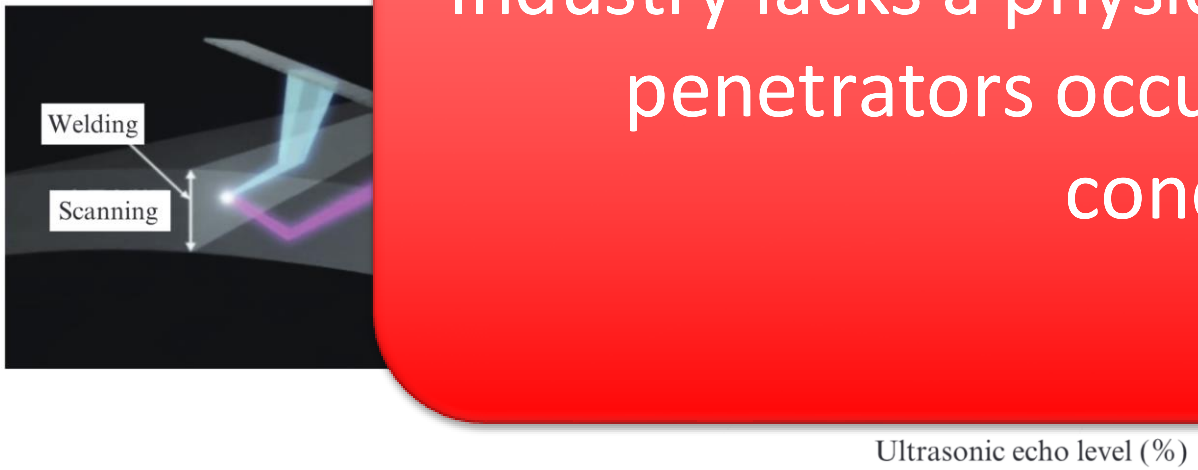

JFE Steel's ultrasonic testing (UT) schematic (left) and correlation between UT echo level and impact toughness.
(T. Okabe, Y. Iizuka, and S. Igi, 2015)

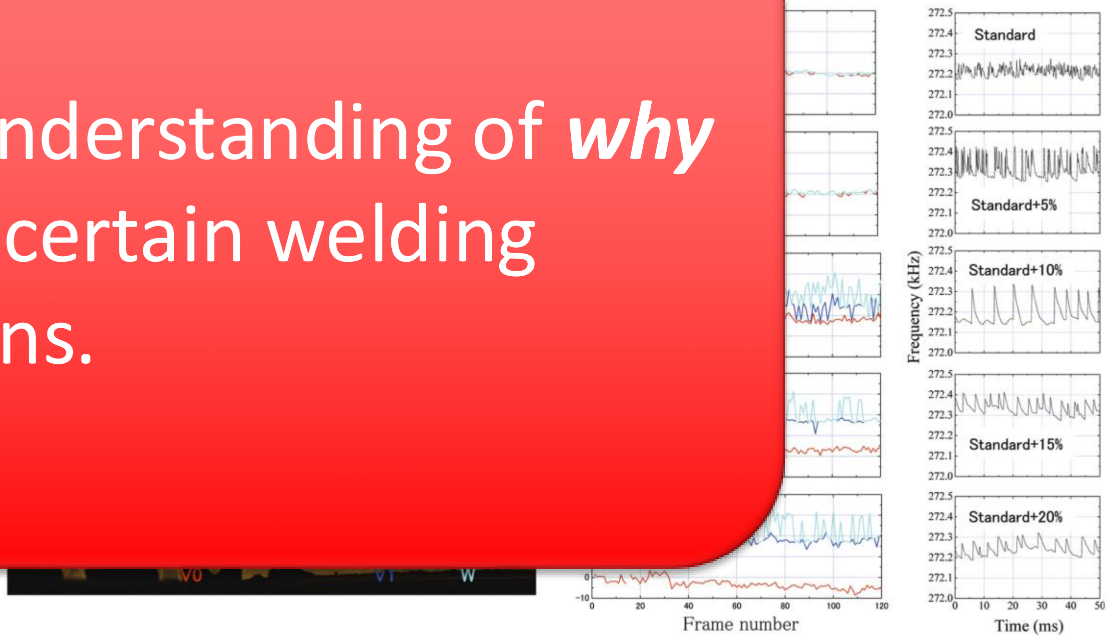

(a) Detected points in various heat input (b) Trend chart of the detected points (c) Frequency waveforms

Nippon's optical and electrical monitoring of 24" pipe .
(N. Hasegawa *et al.*, 2015)

The Process Problem

- ERW community observations:
  - There **is** a molten interface in the vee
  - Molten metal is displaced **prior to squeezing**
  - Potential re-entry of expelled molten metal that oxidized [1-5]
  - Others presume lack of squeeze pressure to eject oxides [6-8]

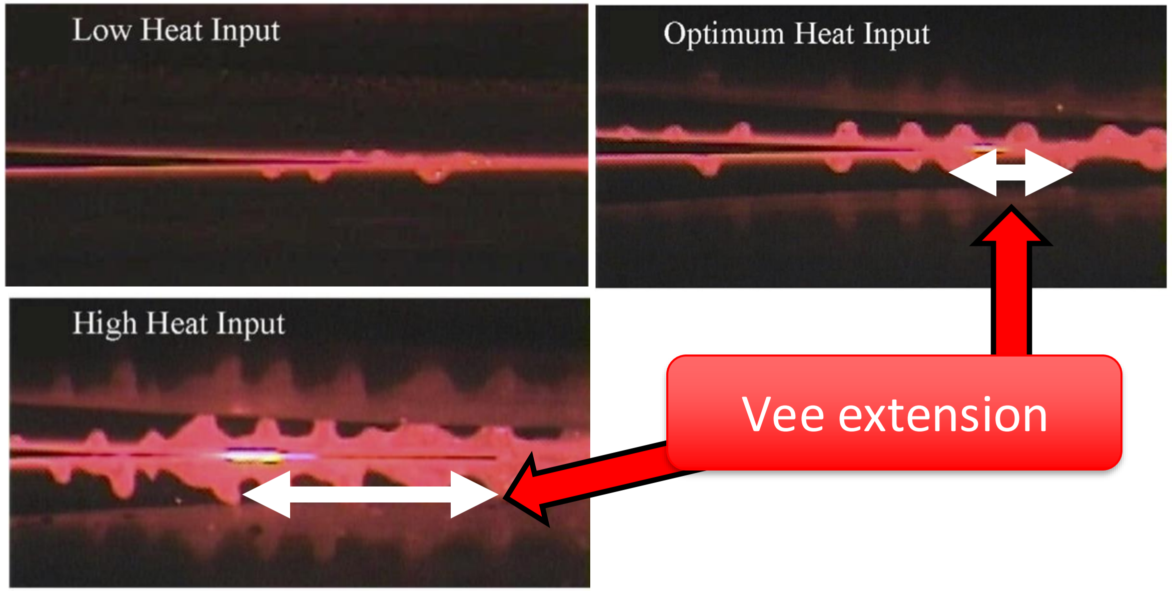

The three general weld conditions observed in-situ.
(C. M. Kim and J. K. Kim, Jan. 2009)

<u>Mechanisms Central To Penetrators</u>

1. **Exposure** of molten metal to atmosphere
2. **Oxidation** of exposed molten metal
3. **Retainment/re-entry** of oxidized material

[1] H. Haga, K. Aoki, and T. Sato, 1981

[2] H. Haga, K. Aoki, and T. Sato, 1980

[3] N. Hasegawa et al., 2015

[4] C. M. Kim and J. K. Kim, Feb. 2009

[5] C. M. Kim and J. K. Kim, Jan. 2009

[6] N. Hasegawa et al., Sep. 2012

[7] T. Inoue, M. Suzuki, T. Okabe, and Y. Matsui, 2013

[8] T. Okabe, Y. Iizuka, and S. Igi, 2015

Project Objectives and Scope

Mechanisms Central To Penetrators

1. **Exposure** of molten metal to atmosphere
2. **Oxidation** of exposed molten metal
3. **Retainment/re-entry** of oxidized material

Encapsulating Hypothesis

The removal and/or control of at least one of the three central mechanisms will directly prevent penetrators.

- Develop mechanistic **understanding** of ERW and penetrators
- Use **direct observations** to rank key mechanisms and validate modelling

Key Principles

- Material chemistry
- Heat transfer
- Fluid mechanics of molten metal
- Plastic flow
- Oxidation thermodynamics and kinetics
- Weld interface quality

High Level Effects of Process Parameters

- Increasing heat input…
  1. Widens & lengthens vee extension
  2. Increases average penetrator length

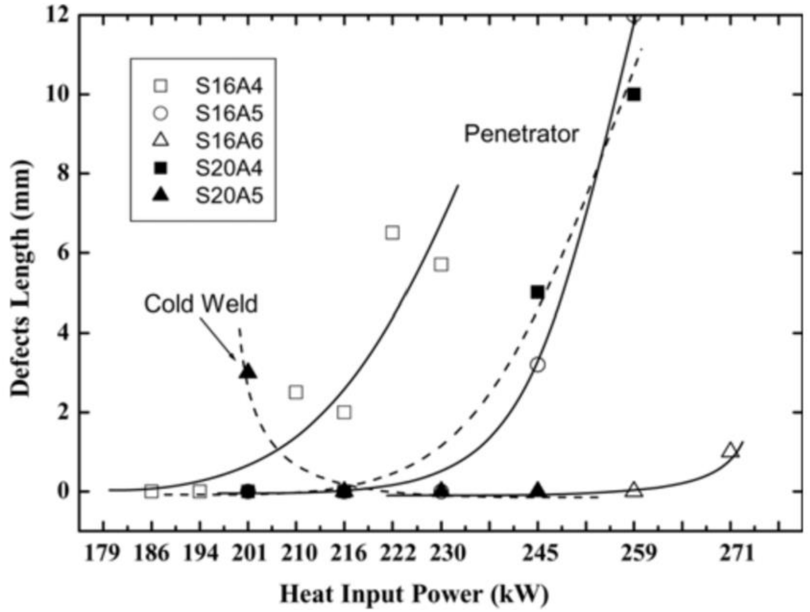

Parametric study to determine the effect of heat input on defects.
(C.-M. Kim and J.-K. Kim, Feb. 2009)

- Increasing vee angle…
  – Increases *vee convergence*
  – Decreases vee extension length at fixed heat input

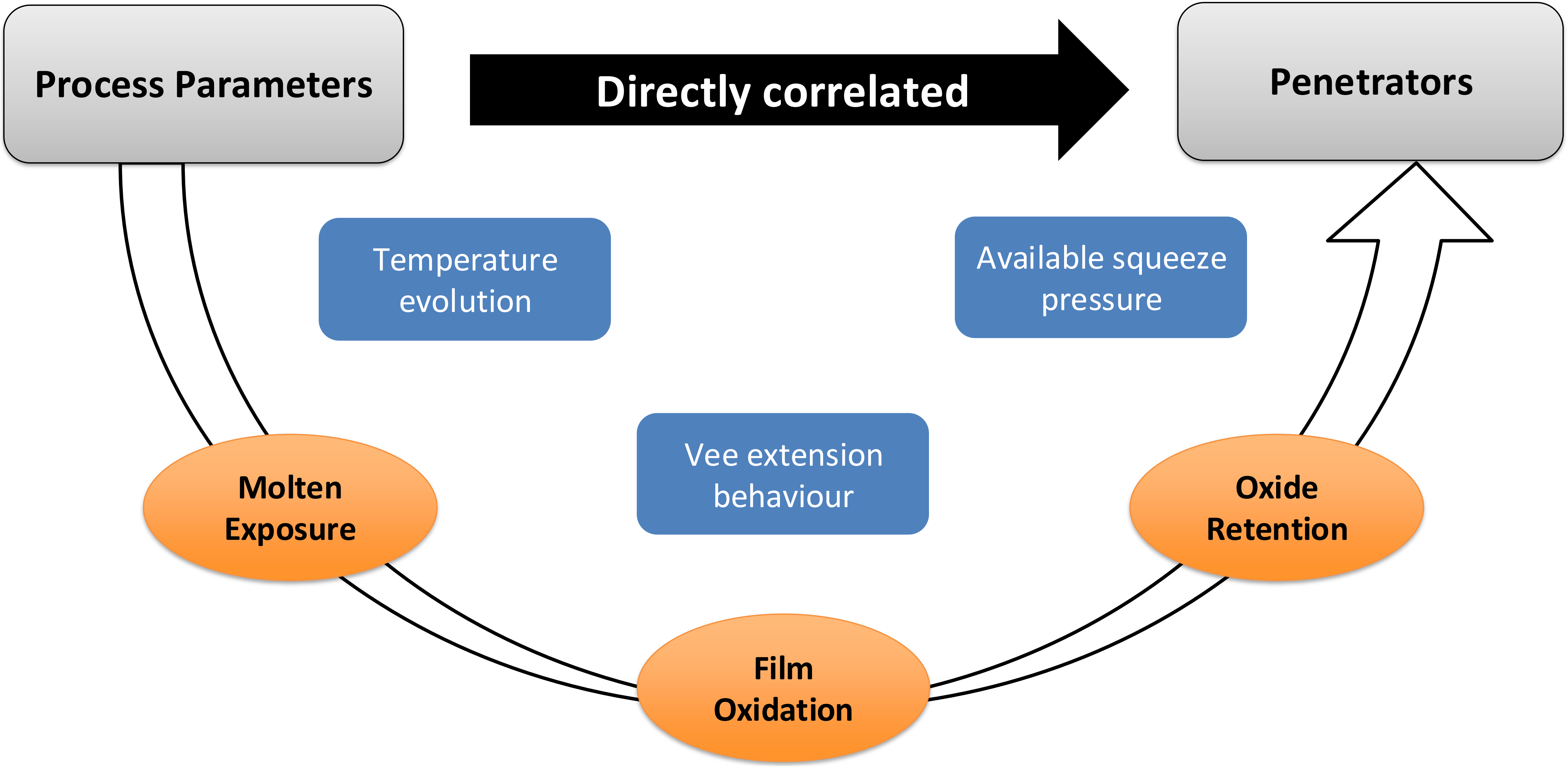
Process Parameters
Directly correlated
Penetrators
Temperature evolution
Available squeeze pressure
Vee extension behaviour
Molten Exposure
Oxide Retention
Film Oxidation

Fundamental Concepts

Key Concept: Process Regimes

- Dimensionless ratios
- Thermal depth vs power depth
  - Can be used to predict temperature behaviour

$$\delta_{\mathrm{T}} = \sqrt{\frac{4\alpha x}{\pi U}}$$

$$\delta_{\mathrm{P}} = \frac{1}{2\sqrt{\pi f \mu \sigma}}$$

$$\delta^* = \frac{\delta_{\mathrm{T}}}{\delta_{\mathrm{P}}}$$

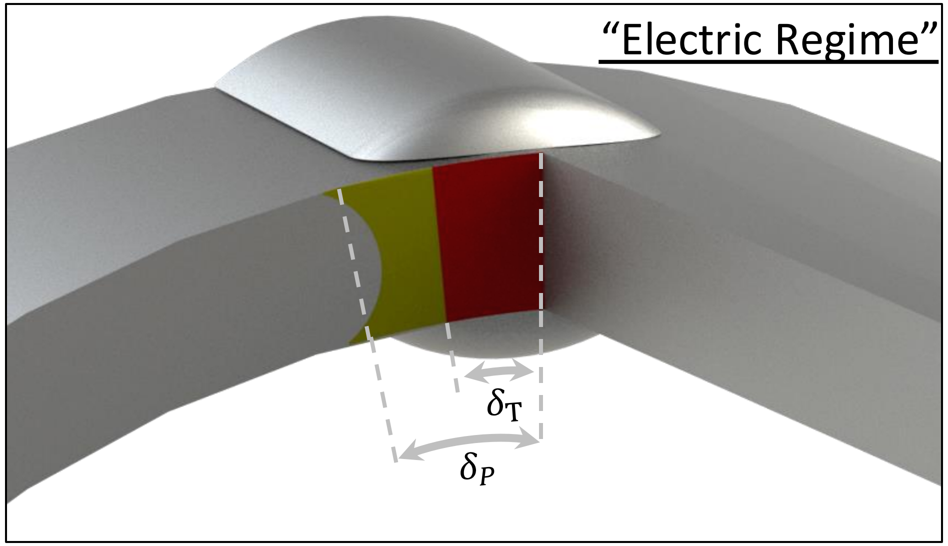

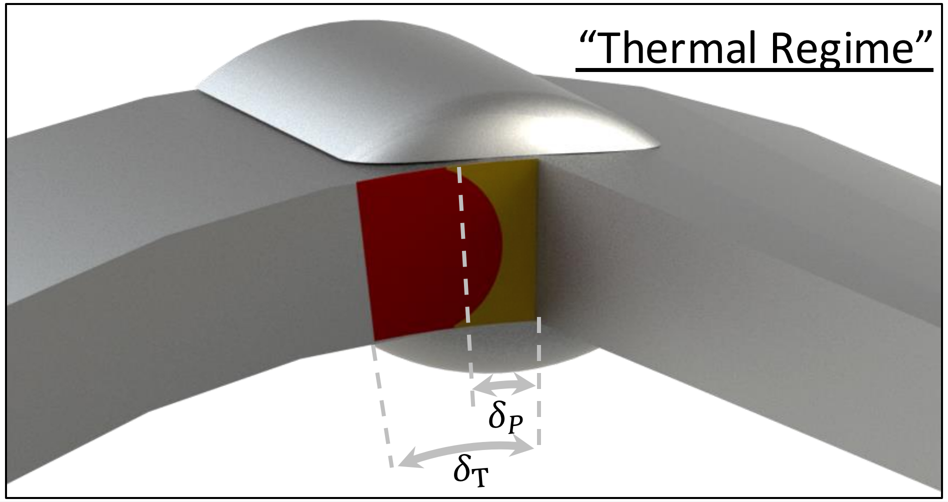

Ejection of Molten Metal

- Intense Lorentz forces expel molten material out of the vee **prior to upsetting**
- Net effect is characterized as ***ablation***
  - The **removal** of mass that reaches a critical temperature
  - In ERW, this temperature is **melting**

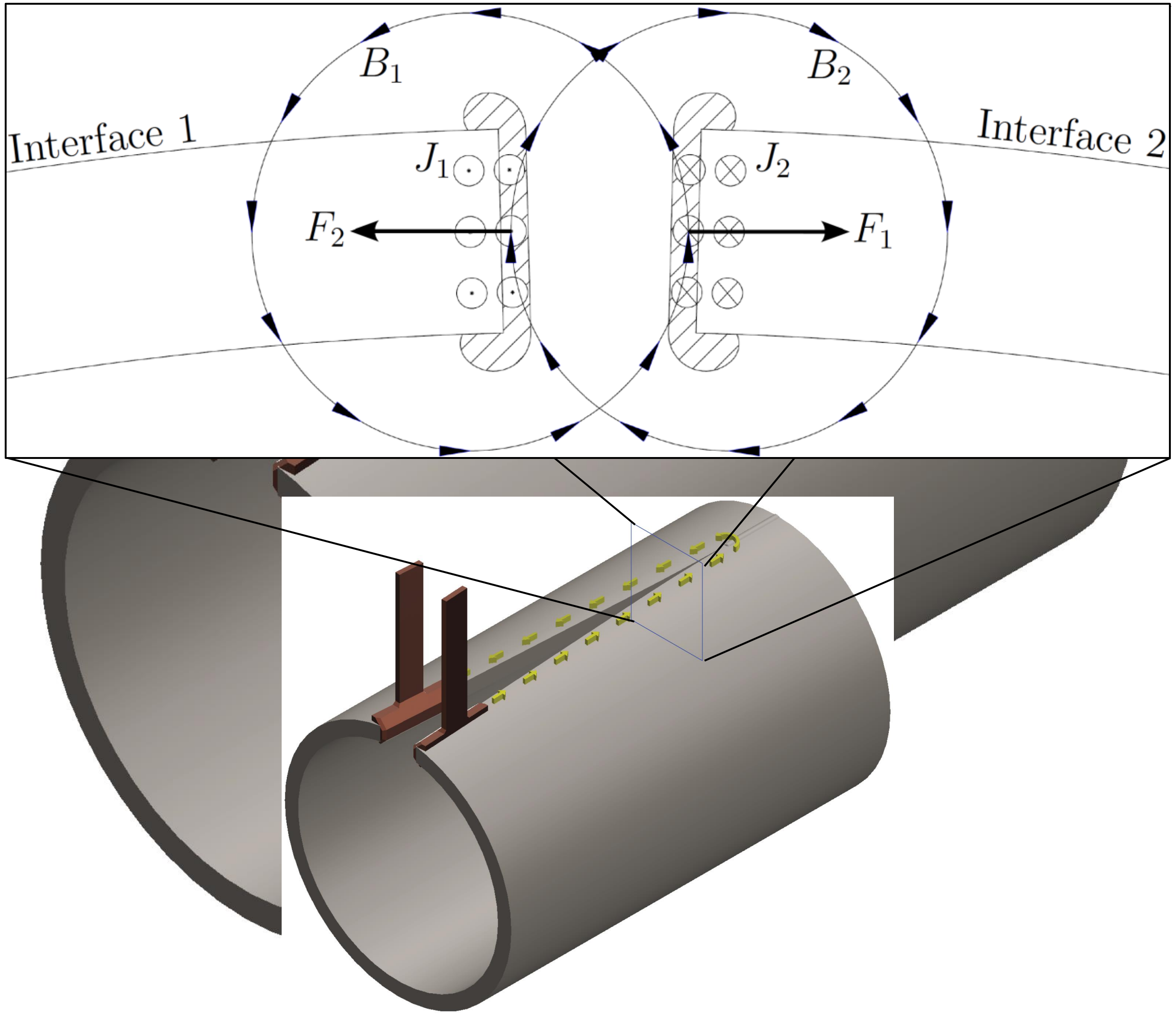

Analysis of Ejection Mechanisms

General Heat Model

$$0 = k\frac{\partial^2 T}{\partial y^2} - \rho c_p U_x \frac{\partial T}{\partial x} + q_g'''$$

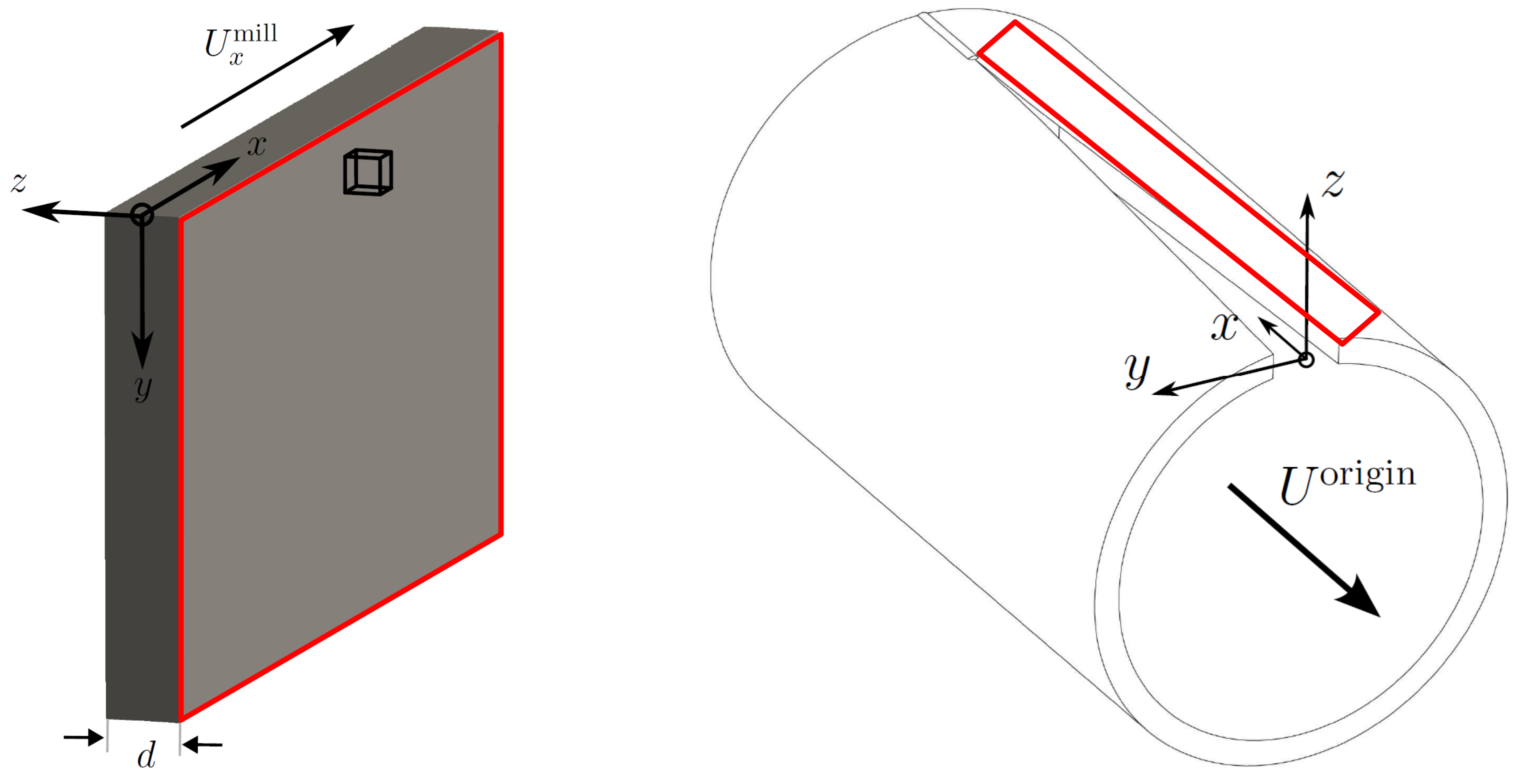

The Heat Model Solution

- Full temperature field $\theta(x,y)$ solution

$$T(x,y)-T_0=\frac{q_0'''\delta_P^2}{k}\left[\sqrt{\frac{4\alpha x}{\pi U\delta_P^2}}\exp\left(-\frac{y^2}{\frac{4\alpha x}{U}}\right)-\frac{y}{\delta_P}\operatorname{erfc}\left(\frac{y}{\sqrt{\frac{4\alpha x}{U}}}\right)-\exp\left(\frac{y}{\delta_P}\right)+\frac{1}{2}\exp\left(\frac{\alpha x}{U\delta_P^2}-\frac{y}{\delta_P}\right)\operatorname{erfc}\left(\sqrt{\frac{4\alpha x}{\pi U\delta_P^2}}-\frac{y}{\sqrt{\frac{4\alpha x}{U}}}\right)+\frac{1}{2}\exp\left(\frac{\alpha x}{U\delta_P^2}+\frac{y}{\delta_P}\right)\operatorname{erfc}\left(\sqrt{\frac{4\alpha x}{\pi U\delta_P^2}}+\frac{y}{\sqrt{\frac{4\alpha x}{U}}}\right)\right]$$

- Weld surface (bond-plane) solution

$$T(x,y)=T_0+\frac{I^2}{4\sigma k d^2}\,\mathrm{F}\left(\frac{\delta_T}{\delta_P}\right)$$

$$\delta_T=\sqrt{\frac{4\alpha x}{\pi U}}$$

$$\delta_P=\frac{1}{\sqrt{4\pi f\mu\sigma}}$$

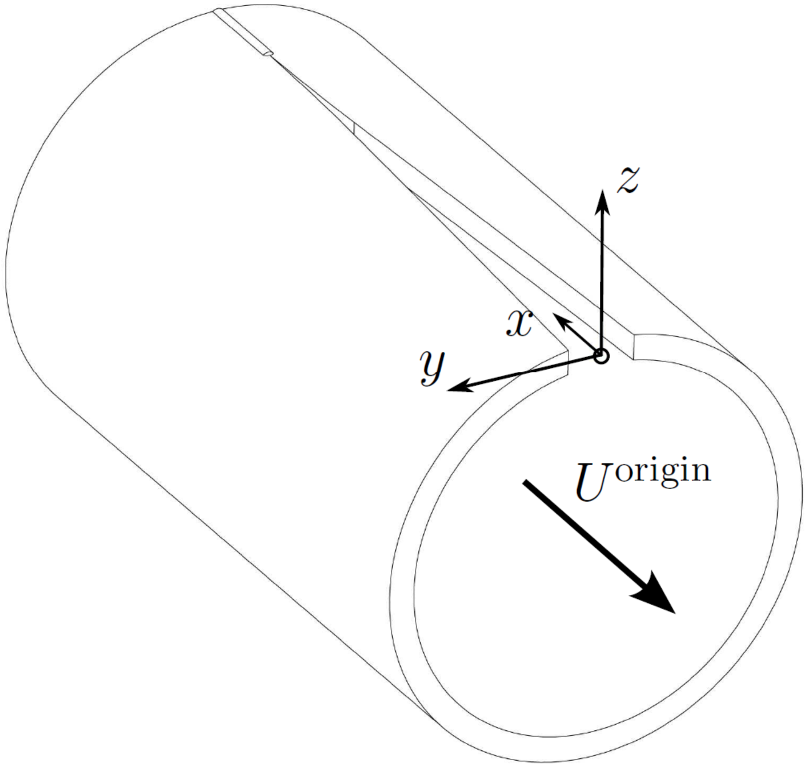

Defining The Vee

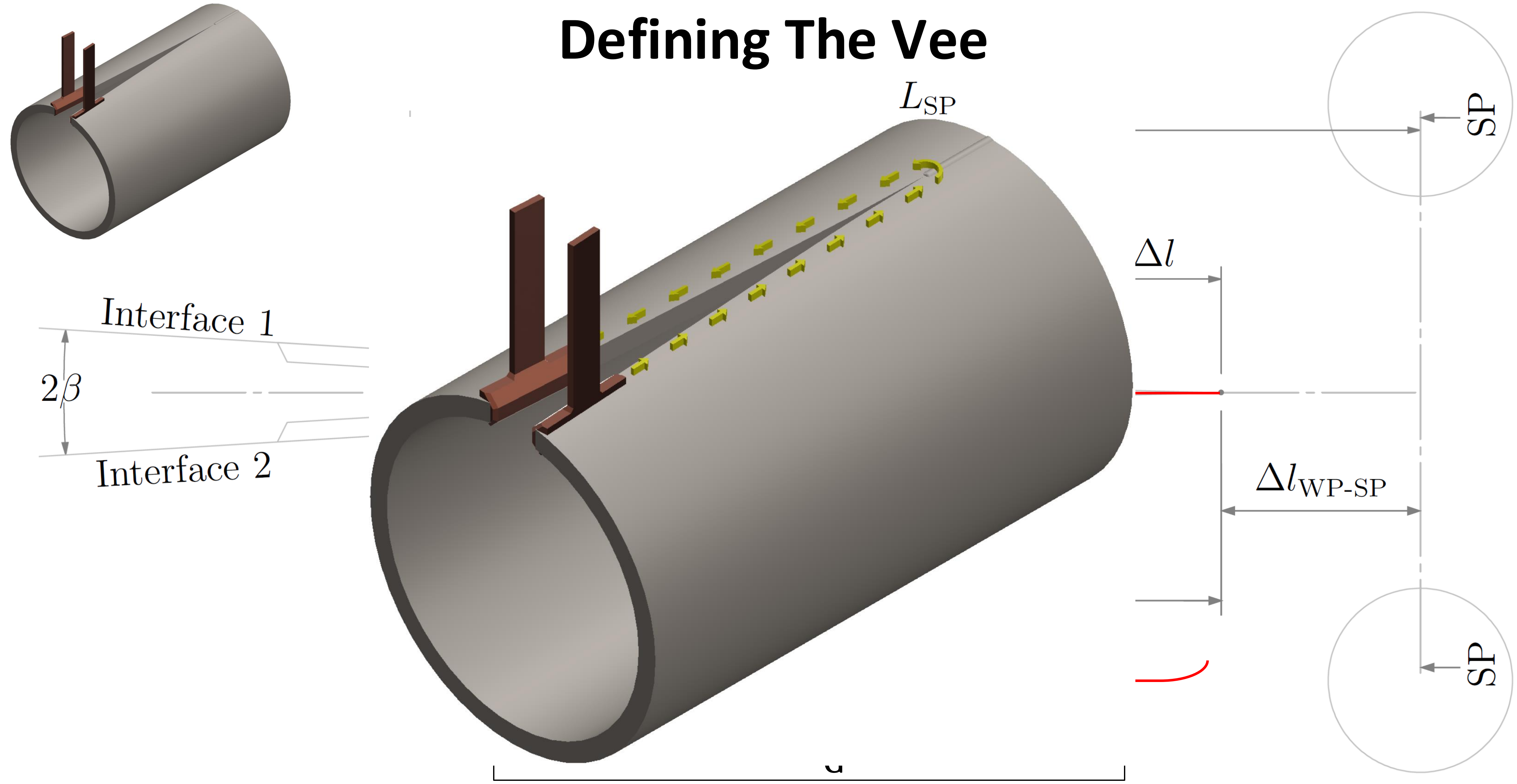

Vee Length Extension Model

- Bounding equations:

Temperature field

Ablation effects

Interface conjoining on principle axis

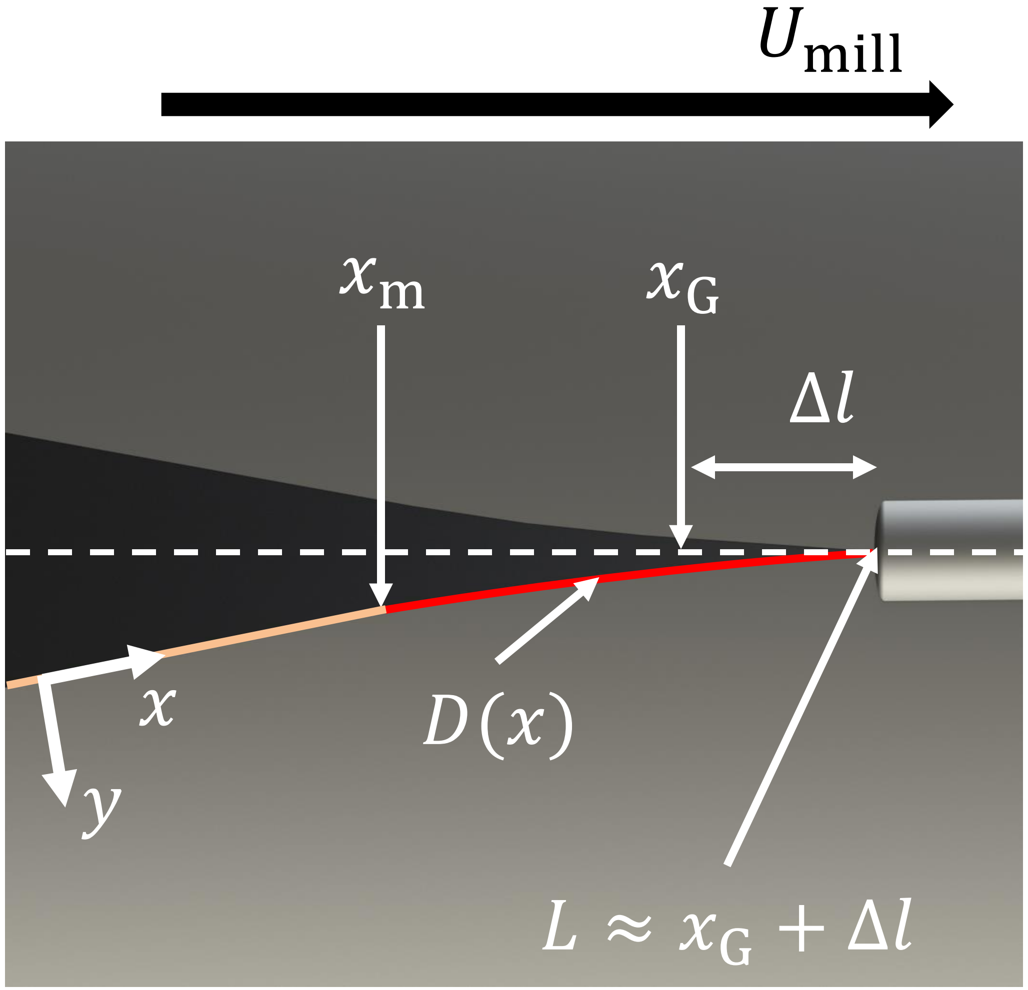

Results

- Validated used two independent datasets from legacy publications
  - (Haga et al., 1980) reported vee extensions from high-speed videographic trials
  - (Scott, 1996) intentionally conducted trials with zero vee extension
- Recall model assumptions

∴ My model enables the prediction weld zone temperature AND physical behaviour.

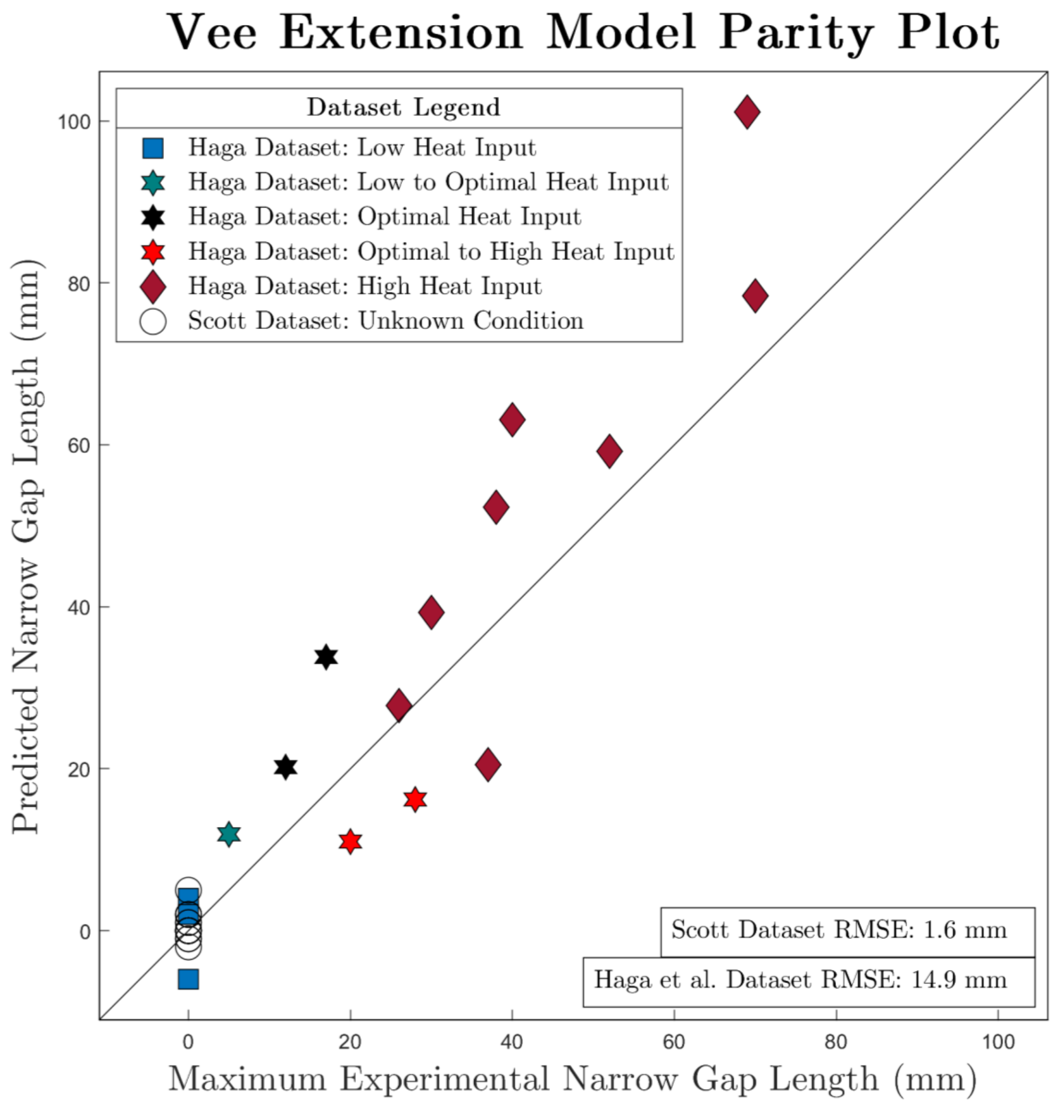

Significance of the Model

Why determine *melting onset* and *vee extension* ???

Answer:

Systematic process characterization

Intermediate Calculation	Physically Significant Tool
• Transient characteristic time t_C^* • Distance between x_m and x_G	The stability of a process' weld zone location
Distance between x_m and WP	Exposure time of molten metal in atmosphere
Distance between WP and SP	Available squeeze pressure due to ablated material

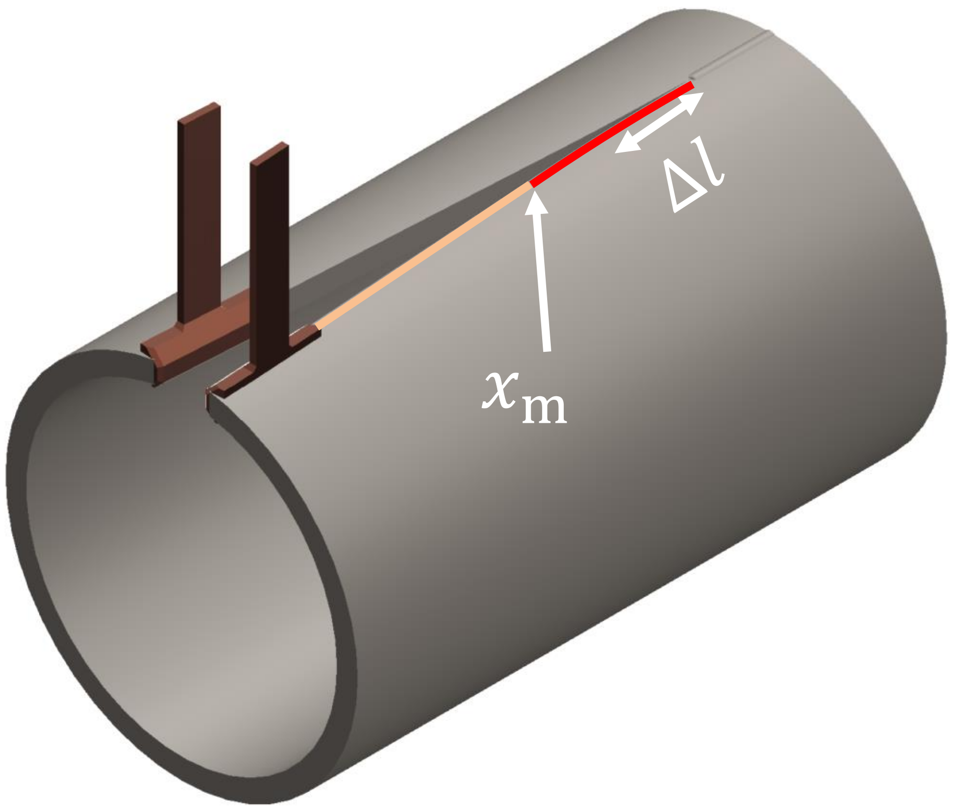

Integration of Insights

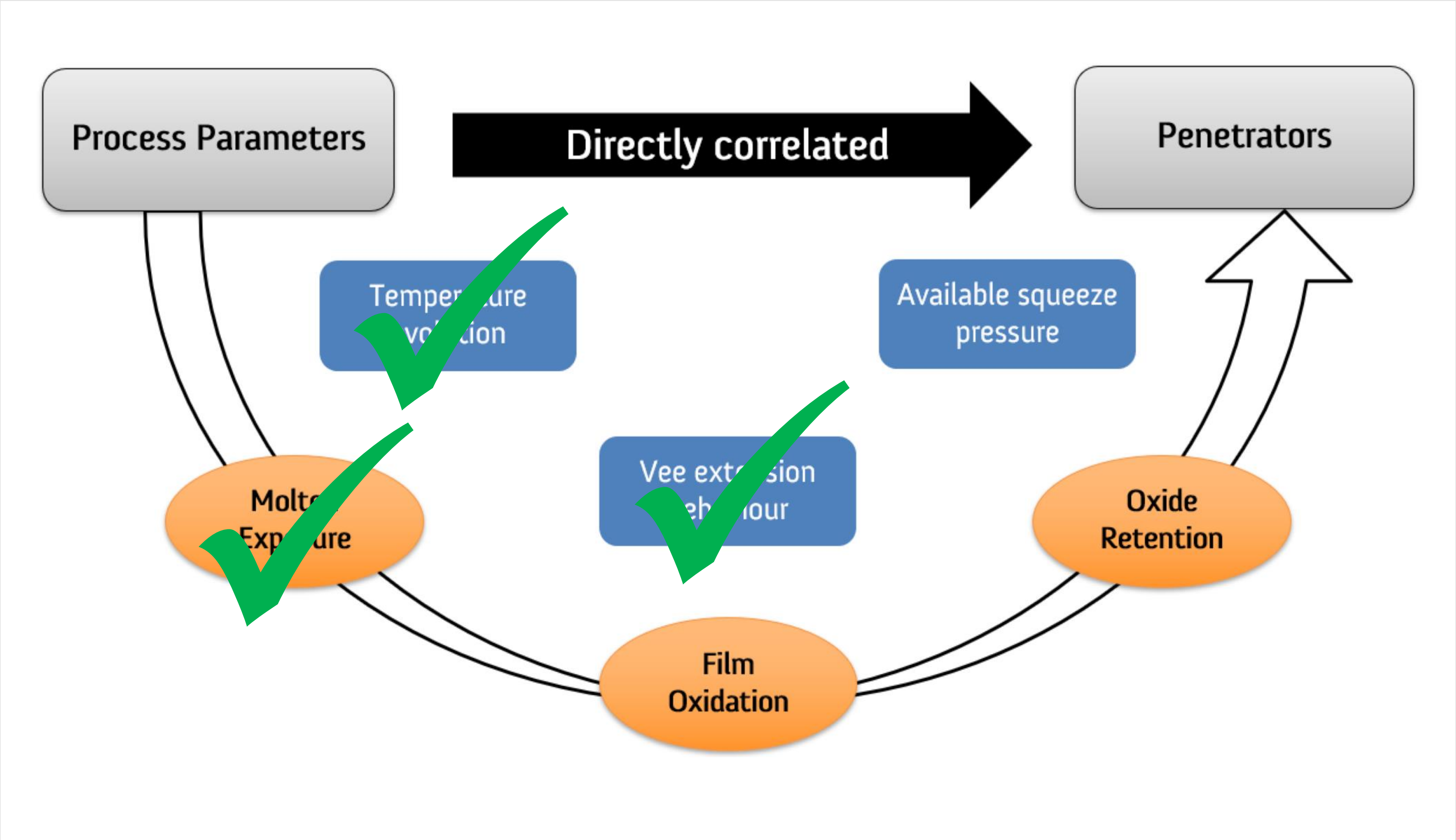

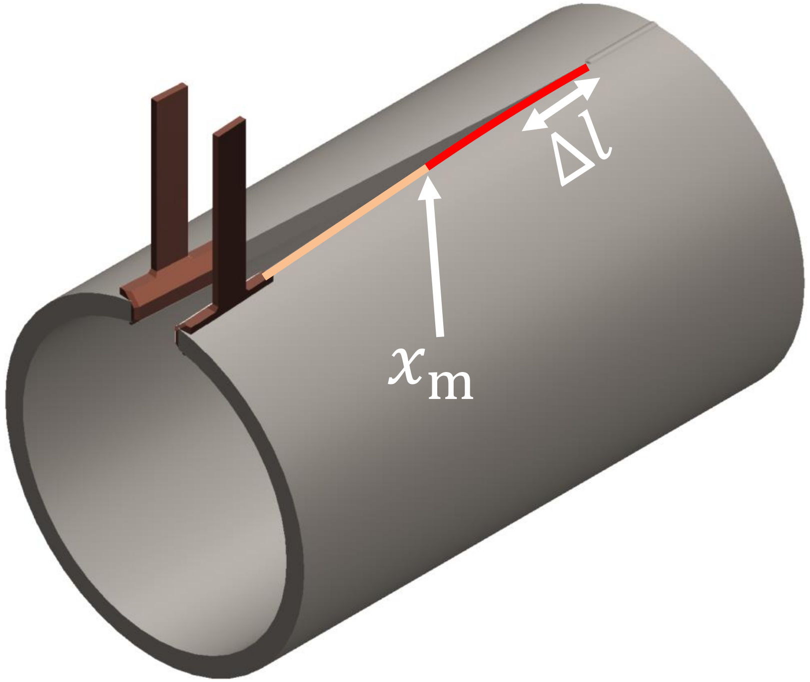

Physically Significant Tool
✓ The stability of a process' weld zone location.
✓ Exposure time of molten metal in atmosphere.
Available squeeze pressure due to ablated material.

Final Remarks

Final remarks

Summary

- Industry lacks a physical understanding of ***why*** penetrators occur at certain welding conditions.
- The current heat transfer – ablation model enables the **quick prediction** of:
  - Melting onset location
  - Vee length response to process parameters
  - Exposure time of molten metal

Future Work

- Analytical expressions for characteristic values will be obtained using blending of asymptotics
- Characteristic value expressions will simplify current vee extension model
- Key physical mechanisms will be identified using high-speed videography and metallographic characterization

Project Sponsor

EVRAZ

North America

Citations

C. M. Kim and J. K. Kim, “The effect of electromagnetic forces on the penetrator formation during high-frequency electric resistance welding,” J Mater Process Technol, vol. 209, no. 2, pp. 838–846, Jan. 2009, doi: 10.1016/J.JMATPROTEC.2008.02.079

H. U. Hong, J. B. Lee, and H. J. Choi, “Improvement of resistance to hydrogen induced cracking in electric resistance welded pipes fabricated with slit coils,” Metals and Materials International 2009 15:1, vol. 15, no. 1, pp. 133–139, Feb. 2009, doi: 10.1007/S12540-009-0133-5.

T. Okabe, Y. Iizuka, and S. Igi, “JFE Technical Report No. 20,” in JFE Technical Report, 2015, pp. 125–132

N. Hasegawa et al., “Nippon Steel & Sumitomo Metal Technical Report No. 107,” Feb. 2015

H. Haga, K. Aoki, and T. Sato, “The Mechanisms of Formation of Weld Defects in High-Frequency Electric Resistance Welding,” Weld J, vol. 60, pp. 104–109, Jun. 1981.

H. Haga, K. Aoki, and T. Sato, “Welding Phenomena and Welding Mechanisms in High Frequency Electric Resistance Welding - 1st Report,” Weld J, vol. 59, no. 7, pp. 208–212, Jul. 1980.

N. Hasegawa et al., “Nippon Steel & Sumitomo Metal Technical Report No. 107,” Feb. 2015.

C. M. Kim and J. K. Kim, “The Effect of Heat Input on the Defect Phases in High Frequency Electric Resistance Welding,” Met. Mater. Int, vol. 15, no. 1, pp. 141–148, Feb. 2009, doi: 10.1007/s12540-009-0141-5.

N. Hasegawa et al., “IPC2012-90222 Development of a New Optical Monitoring System of Welding Conditions for Producing HF-ERW Line Pipes With High Weld Seam Toughness: Advanced Welding Process of HF-ERW 2,” in Volume 3: Materials and Joining, Calgary, Alberta, Canada: American Society of Mechanical Engineers, Sep. 2012, pp. 237–245. doi: 10.1115/IPC2012-90222.

T. Inoue, M. Suzuki, T. Okabe, and Y. Matsui, “JFE Technical Report No. 18,” in JFE Technical Report, vol. 18, 2013, pp. 18–22.

P. F. Scott, “A Study of the Key Parameters of High Frequency Welding.” pp. 1–17, 1996.

Thank you

A NOVEL APPROACH TO SOLVING THE ERW WELD ZONE

Daniele D. G. Calista
PhD Candidate CCWJ
University of Alberta

Dr. Greg R. Lehnhoff
Manager, Welding and Testing R&D
EVRAZ – North America

Prof. Umberto Prisco
Associate Professor
University of Napoli Federico II

Prof. Patricio F. Mendez
Director CCWJ
University of Alberta

CANWELD 2024
June 12, 2024

Addenda Slides

Penetrator Morphology

- Pancake-type microscopic entrapped Mn:Si variant oxides
  - Some oxides solidify **after** surrounding metal
- Large penetrators are minimized in theory via eutectic MnO:SiO2 composition
  - But small penetrators have still formed
- Partial pressure of O2 is directly correlated to penetrators

SiO_2 → $MnSiO_3$ → $(Mn,Fe)_2SiO_4$ → Cr_2O_3 → AB_2O_4 → MO → (Mn,Fe)O

A. V. Khvan et al., "Oxide formation during electric resistance welding of low carbon steels," Materials Science and Technology, pp. 1–12, Feb. 2016, doi: 10.1179/1743284715Y.0000000123

Reported penetrator chemical analysis in relation to size.

M. H. Shin, J. M. Han, Y. S. Lee, and H. W. Kang, "Study on Defect Formation Mechanisms in ERW for API Steel," in 10th International Pipeline Conference, Calgary, Alberta, Canada: ASME, Sep. 2014, pp. 1–5

Type	Large	Medium	Small	
Size	≥5 µm	1-6µm	~0.3µm	
			White	Black
Composition Range (wt%)	O: 21-30 % Fe: 63-79 % Mn: 0-7 % Si 0-3 %	O: 7-20 % Fe: 68-87 % Mn: 3-12 % Si: 0-2 %	O: 2-2.4 % Fe: 93-96 % Mn: 2-4 % Si: 0-1 %	O: 7-10 % Fe: 77-88 % Mn: 3-9 % Si: 3-4 %

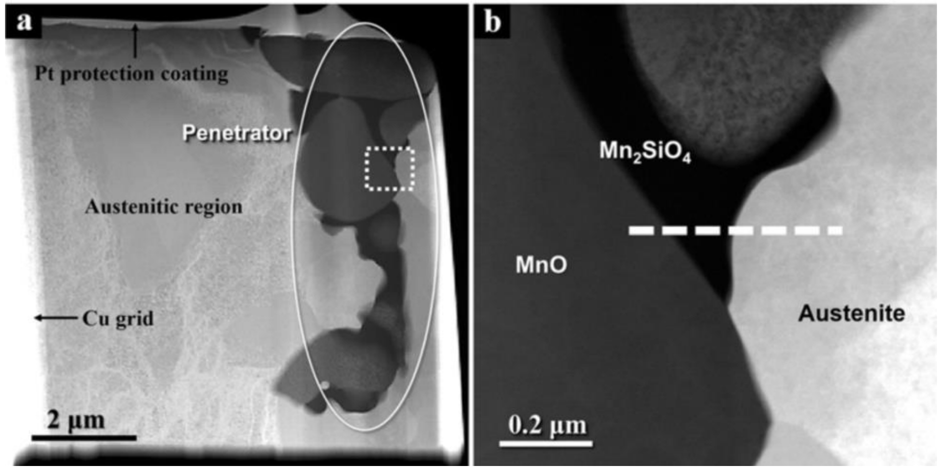

TEM images of a penetrator within a bond line.

G. Park, B. Kim, Y. Kang, H. Kang, and C. Lee, "Characterization of bond line discontinuities in a high-Mn TWIP steel pipe welded by HF-ERW," Mater Charact, vol. 118, pp. 14–21, May 2016, doi: 10.1016/j.matchar.2016.05.005

Molten Bridges: Gap Refilling

- Periodic flashing identified at a fixed point
- Molten metal bridge forms between interfaces immediately after flashing
- Weld point shifts upstream
- Untested theory: Coupled effect of flash frequency and bridge speed

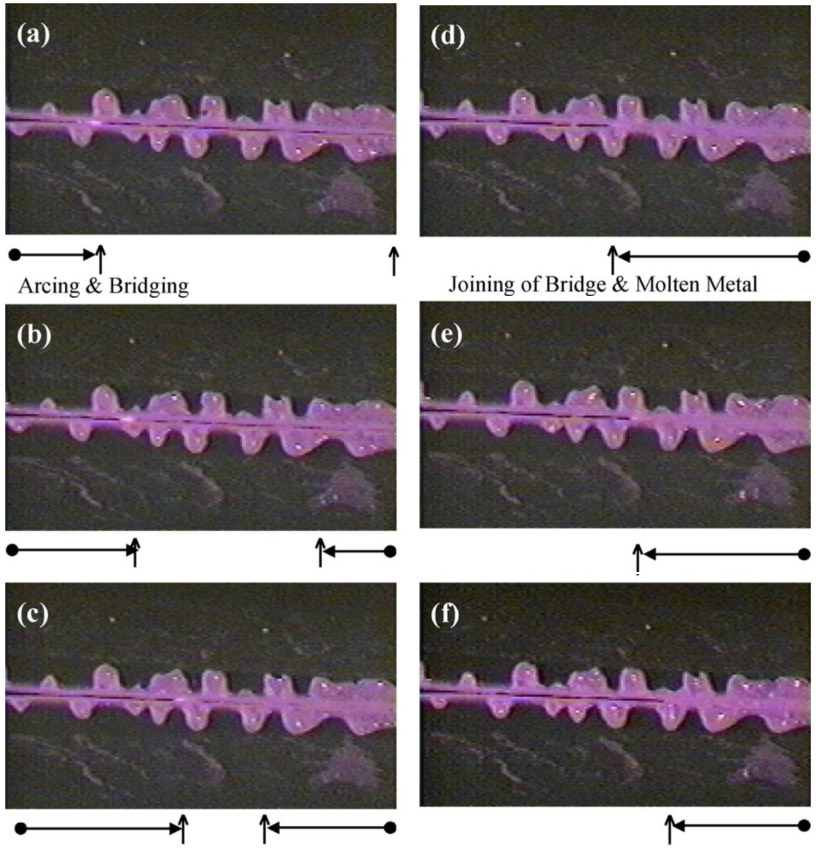

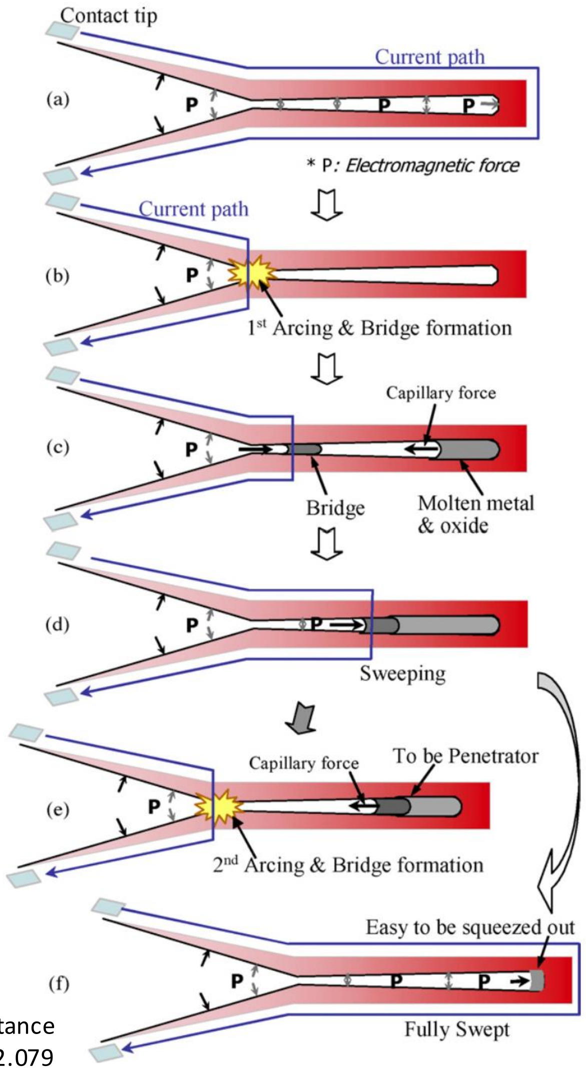

Kim et al.'s observations of arcing, bridge travelling, and weld point movement.

C. M. Kim and J. K. Kim, "The effect of electromagnetic forces on the penetrator formation during high-frequency electric resistance welding," *J Mater Process Technol*, vol. 209, no. 2, pp. 838–846, Jan. 2009, doi: 10.1016/J.JMATPROTEC.2008.02.079

Narrow Gap Effect + Re-Entry of Material

- Periodic flashing identified at a fixed point
- Molten metal bridge forms between interfaces immediately after flashing
- Weld point then shifts upstream
- The cycle repeats for each flash event

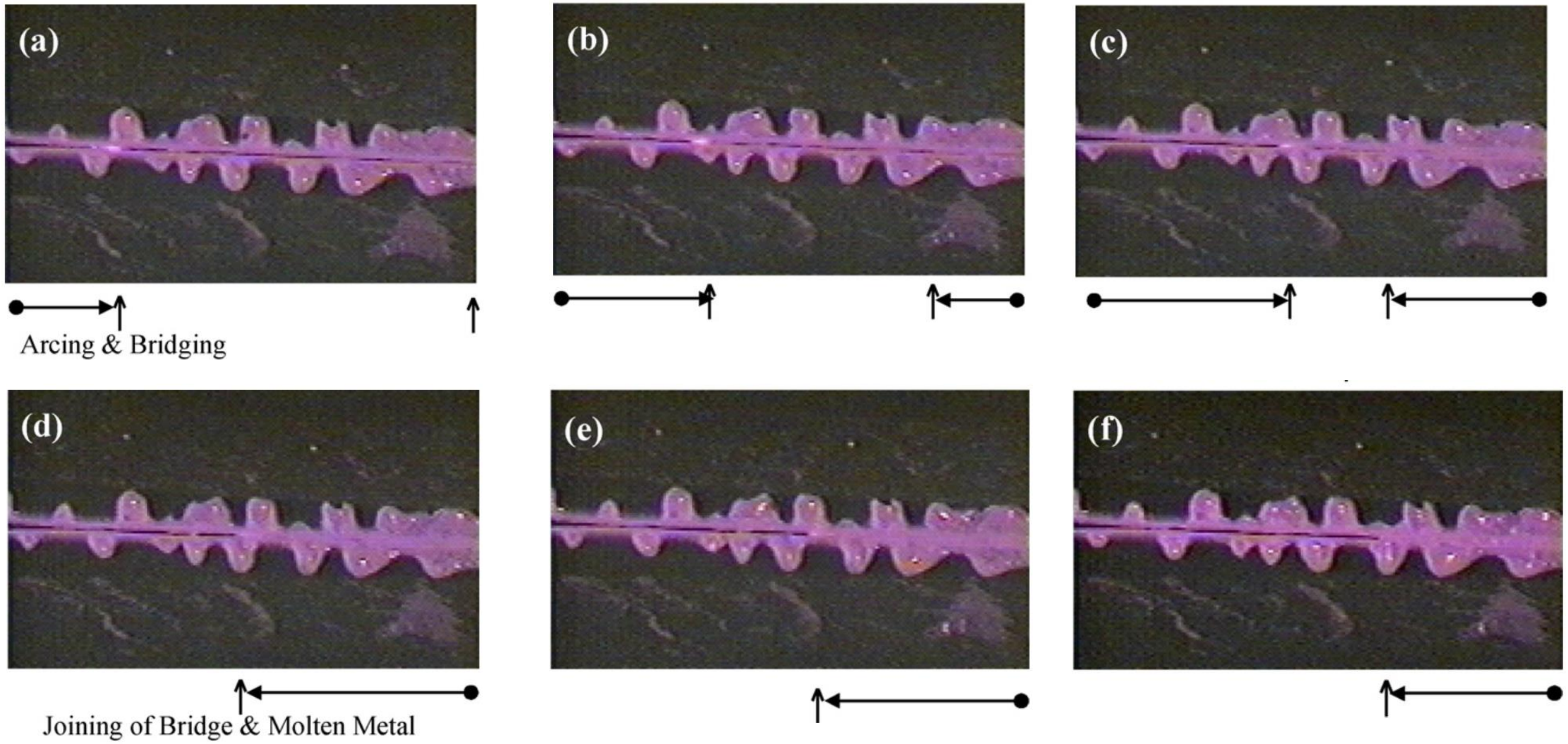

Kim et al.'s observations of arcing, bridge travelling, and weld point movement.

C. M. Kim and J. K. Kim, "The effect of electromagnetic forces on the penetrator formation during high-frequency electric resistance welding," *J Mater Process Technol*, vol. 209, no. 2, pp. 838–846, Jan. 2009, doi: 10.1016/J.JMATPROTEC.2008.02.079

Power Delivered To The Vee

- Recall our assumption of $\frac{\partial q_g'''}{\partial x} = 0$…

$$\therefore q_0''' \approx \frac{P_{vee}}{2d\delta_p(x_G + G)}$$

- To calculate system efficiency*, one **must**:
  - Conduct full scale weld trials designed to force $x_m \approx x_G$, thus $G = 0$.
  - Obtain all RHS parameters in the following:

$$\eta = \frac{P_{vee}}{P_{machine}} = \frac{2\theta_m k d x_G}{\delta_p F(\delta^*) P_{machine}}$$

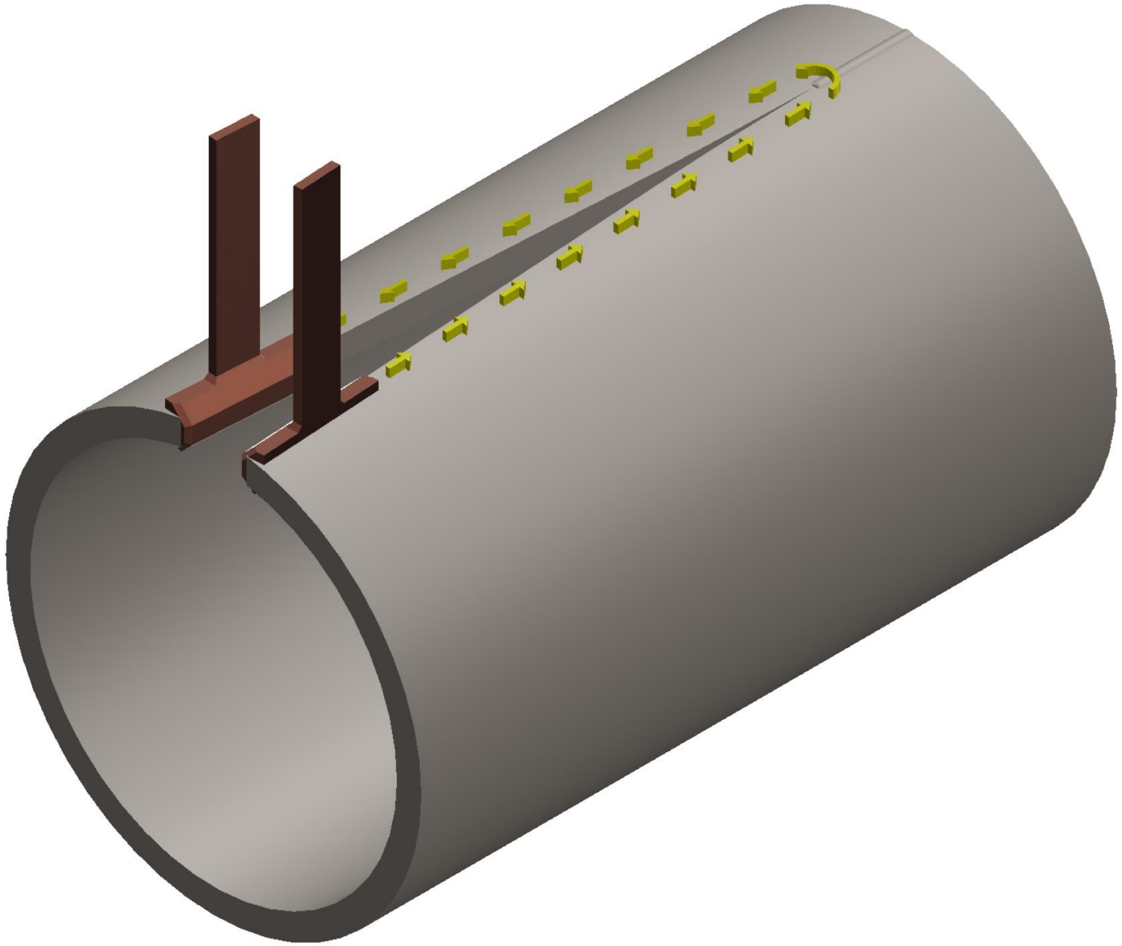

*In the context of this model.

Heat input classifications

- Industry uses arbitrary designations (to date)

- Three Point Concept
  - An attempt at objectively classifying the process into heating regimes
  - Yet to be rigorously explored

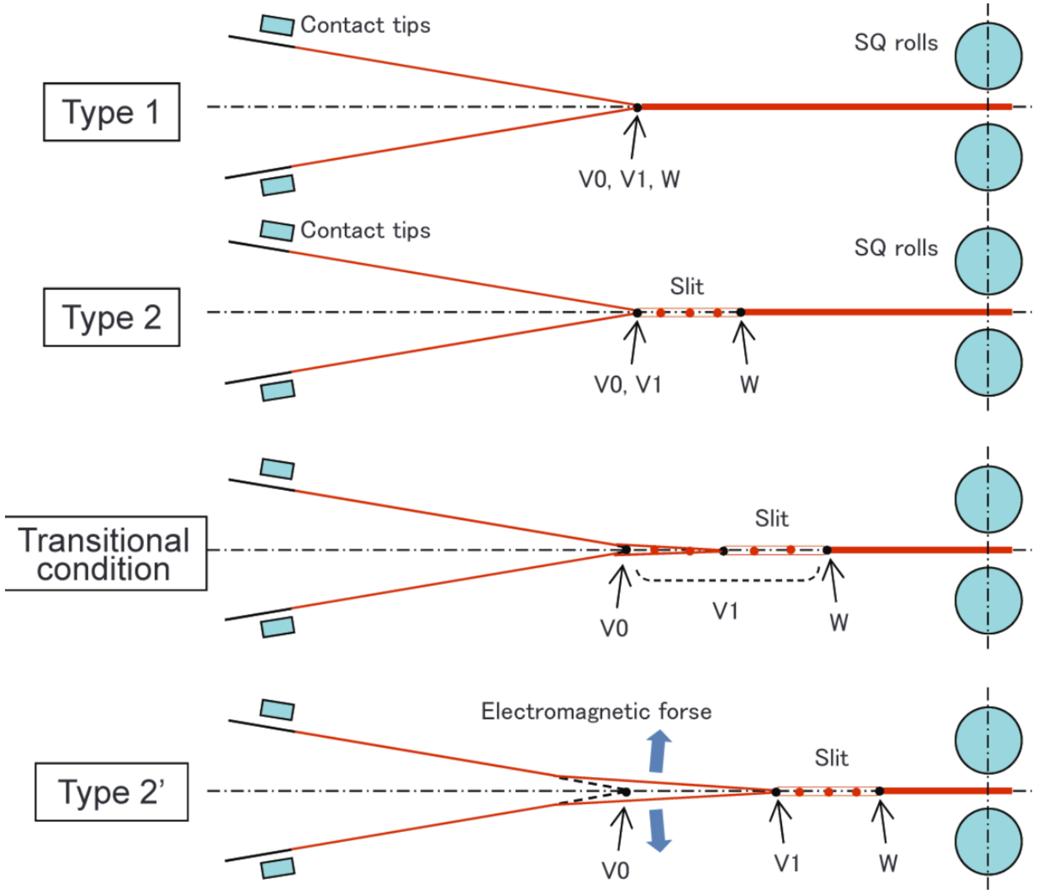

N. Hasegawa *et al.*, "Nippon Steel & Sumitomo Metal Technical Report No. 107," Feb. 2015.

Molten bridges: Flashing and Movement

- Periodic flashing identified at a fixed point
- Molten metal bridge forms between interfaces within 0.1 ms after flashing
- Average velocity is not proportional to heat input
- Sweep length is not consistent
  - Infers changing narrow gap length and a potentially non-stationary weld point

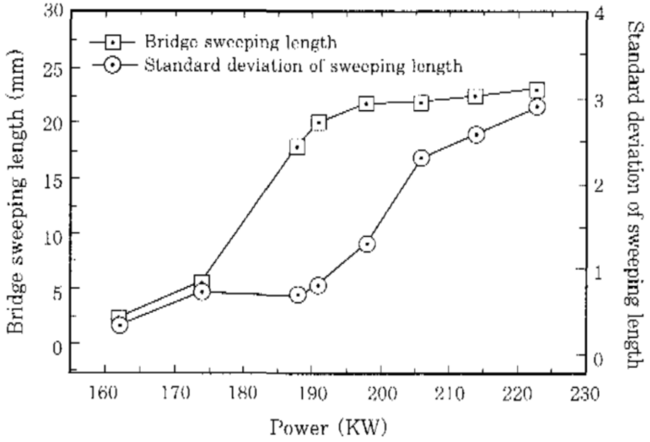

Figure 6 – Measured bridge length and bridge length deviation against heat input (Choi et al., 2001).

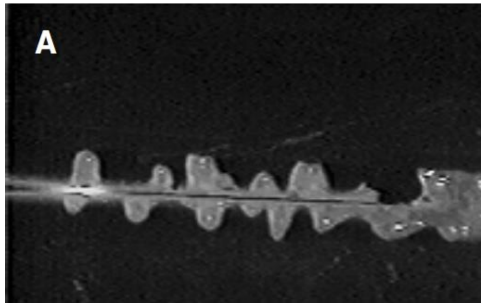

Figure 4 – A flashing event in ERW (Choi et al., 2001).

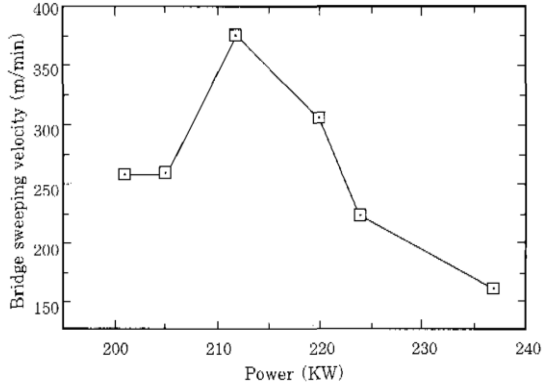

Figure 5 – Measured bridge velocity against heat input (Choi et al., 2001).

- Since more defects are noticed at higher heat inputs, bridge sweeping is critical to understanding penetrators
- Heat input is not a viable variable to develop a model
  - More detailed variables such as current density are necessary

Current distribution

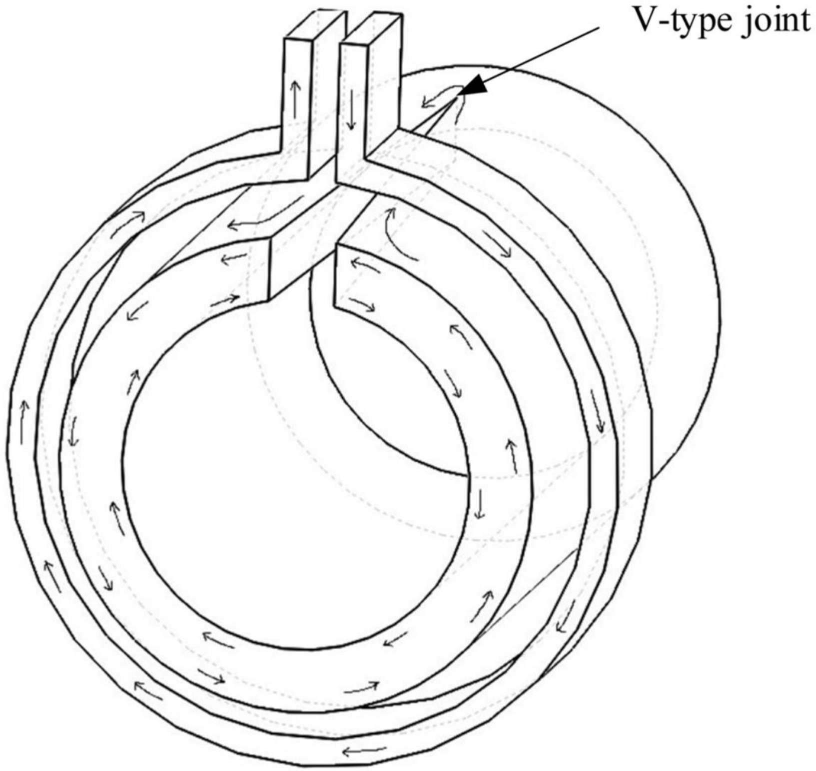

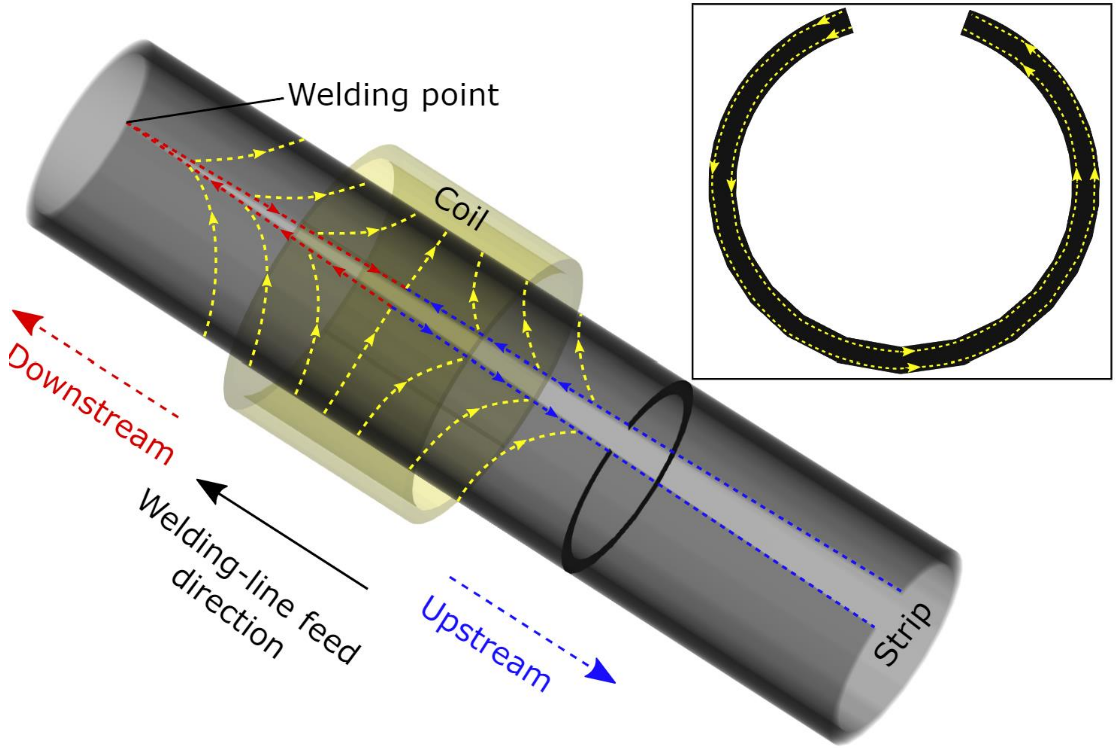

C. Kang *et al.*, "Research on the optimization of welding parameters in high-frequency induction welding pipeline," *J Manuf Process*, vol. 59, pp. 1526–6125, 2020, doi: 10.1016/j.jmapro.2020.10.021.

J. I. Asperheim, P. Das, B. Grande, D. Hömberg, and T. Petzold, "Numerical simulation of high-frequency induction welding in longitudinal welded tubes," Berlin, 2019. doi: 10.20347/WIAS.PREPRINT.2600.

Skin Effect

Current Density Distribution

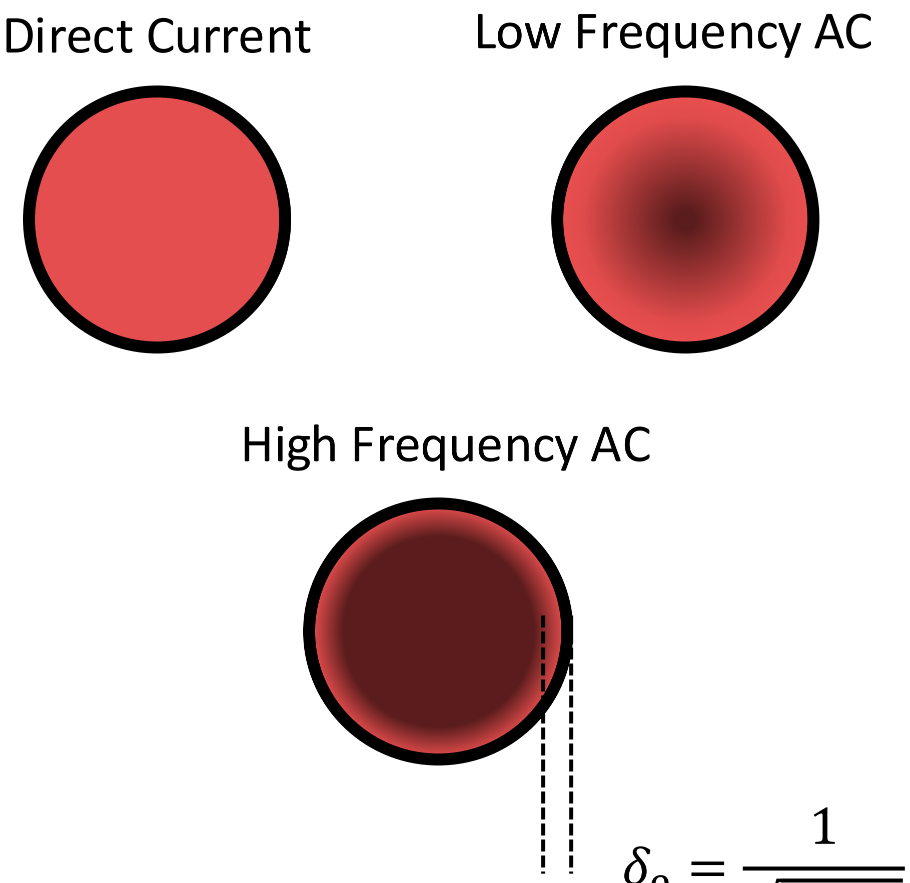

$$\delta_e = \frac{1}{\sqrt{\pi f \mu \sigma}}$$

- Natural phenomena that concentrates current density as frequency ↑
- Helps localize heating and increase melting efficiency
- Key notion: AC current density decays into a conductor

$$J = J_0 \exp\left(-\frac{y}{\delta_e}\right)$$

- Skin depth (δ_e) represents when $\frac{J(\delta_e)}{J_0} = e^{-1}$

General Heat Model

$$0 = k\frac{\partial^2 T}{\partial y^2} - \rho c_p U_x \frac{\partial T}{\partial x} + q_{\mathrm{g}}'''$$

- Hypotheses
  - Neglect thermophysical property temperature dependence
  - Neglect Curie temperature effects
  - $q_{\mathrm{g}}''' \gg k\frac{\partial^2 T}{\partial z^2}$ and $\frac{\partial q_{\mathrm{g}}'''}{\partial x} = 0$
- Conditions
  - Steady-state with respect to electrical coils/contacts
  - $\mathrm{Pe}_x \gg 1$
  - Joule heating is primary heating mechanism

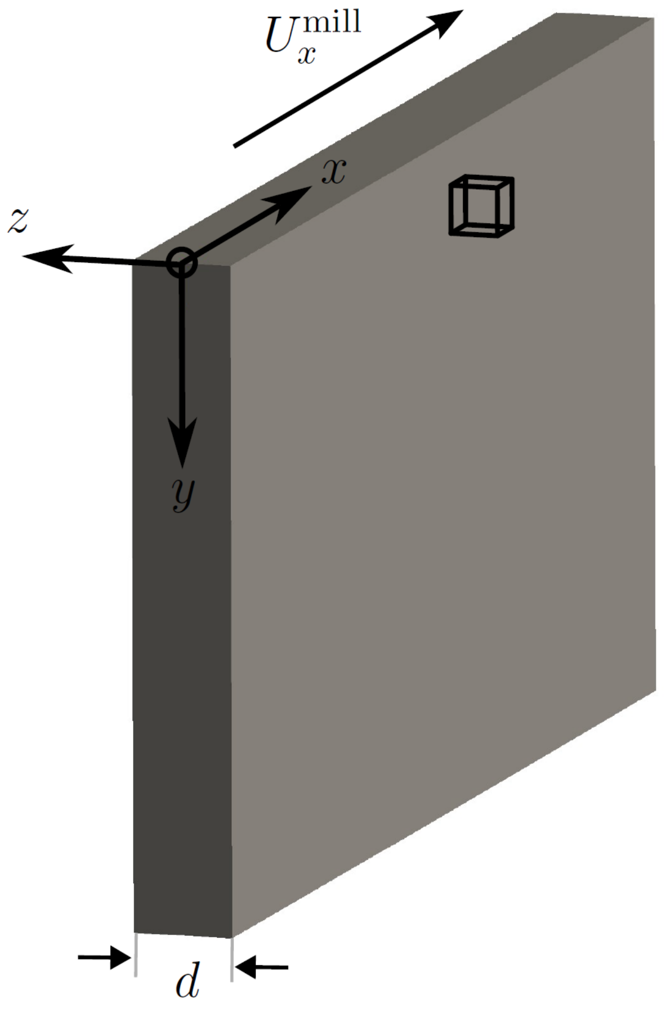

Asymptotic Insights on Weld Surface

$$\theta^* = \frac{4\sigma k d^2}{I^2}\theta$$

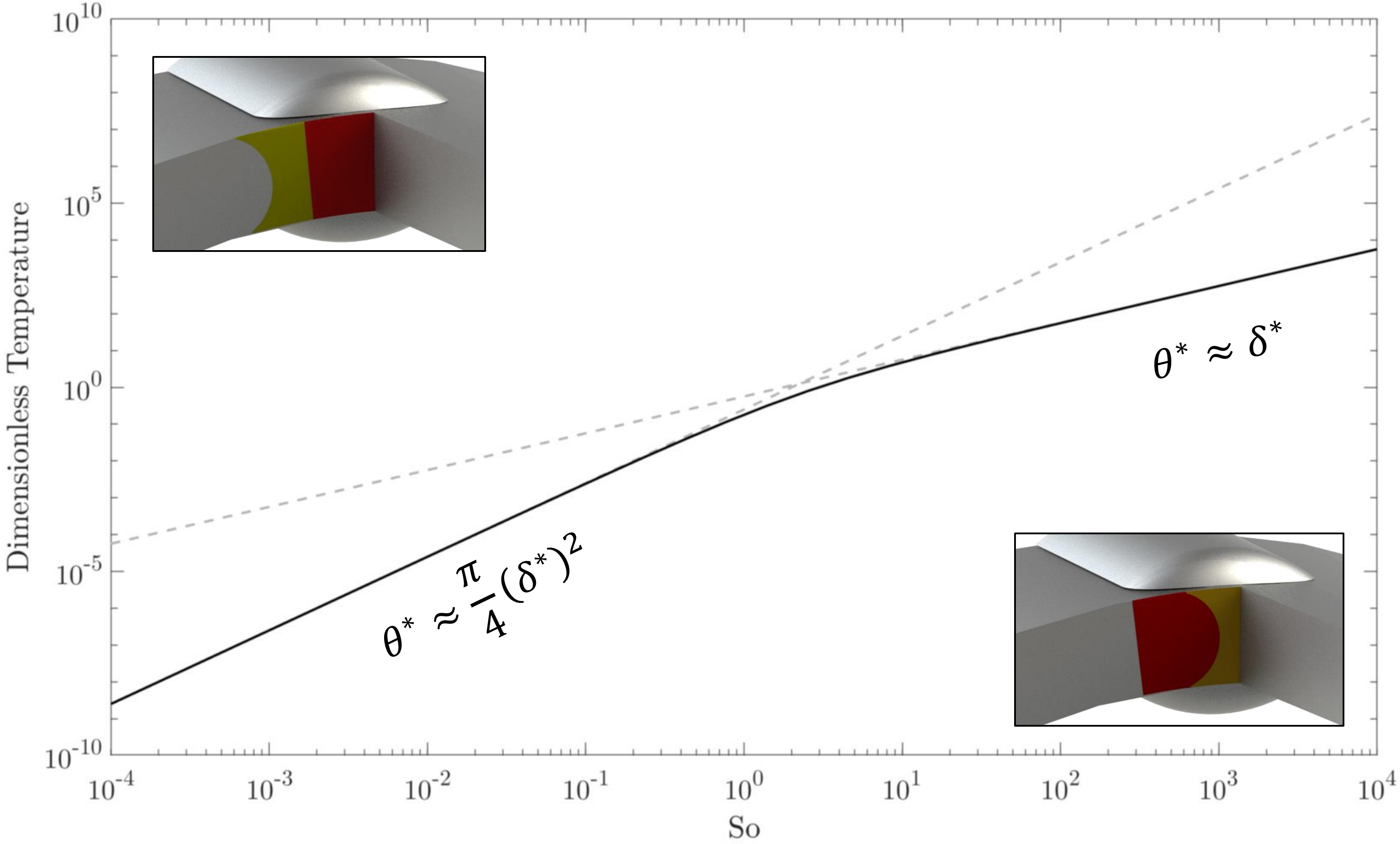

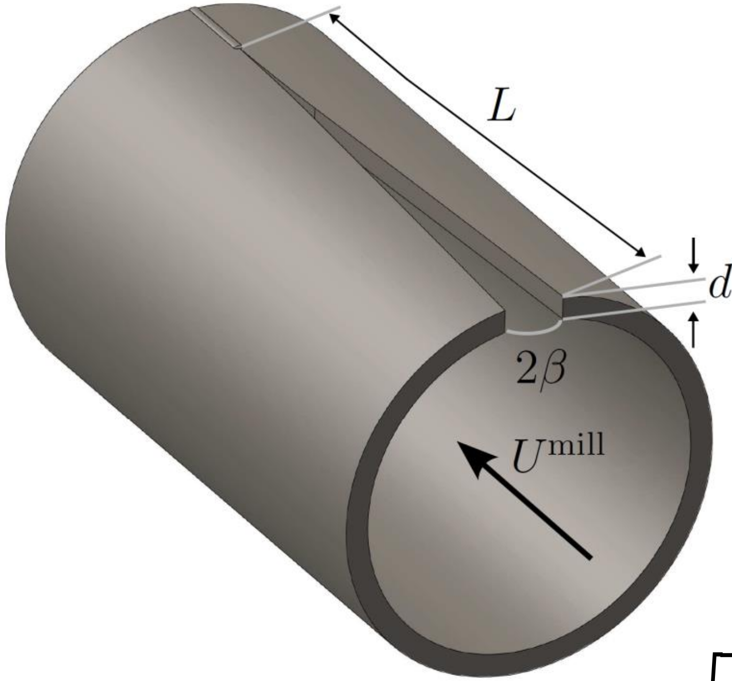

$$\delta_T = \sqrt{\frac{4\alpha x}{\pi U}}$$

$$\delta^* = \frac{\delta_T}{\delta_P}$$

$$\delta_P = \frac{1}{\sqrt{4\pi f \mu \sigma}}$$